bioRxiv preprint doi: https://doi.org/10.1101/2022.05.26.493517; this version posted May 26, 2022. The copyright holder for this preprint (which was not certified by peer review) is the author/funder. All rights reserved. No reuse allowed without permission.

SARS-CoV-2 Omicron BA.2.12.1, BA.4, and BA.5 subvariants evolved to extend antibody evasion

Qian Wang[1*], Yicheng Guo[1*], Sho Iketani[1,2], Zhiteng Li[1], Hiroshi Mohri[1], Maple Wang[1], Jian Yu[1], Anthony D. Bowen[1,3], Jennifer Y. Chang[3], Jayesh G. Shah[3], Nadia Nguyen[1], Kathrine Meyers[1,3], Michael T. Yin[1,3], Magdalena E. Sobieszczyk[1,3], Zizhang Sheng[1], Yaoxing Huang[1], Lihong Liu[1#], and David D. Ho[1,2,3#]

[1]Aaron Diamond AIDS Research Center, Columbia University Vagelos College of Physicians and Surgeons, New York, NY, USA.

[2]Department of Microbiology and Immunology, Columbia University Vagelos College of Physicians and Surgeons, New York, NY, USA.

[3]Division of Infectious Diseases, Department of Medicine, Columbia University Vagelos College of Physicians and Surgeons, New York, NY, USA.

*Equal contribution

[#]Address correspondence to Lihong Liu (ll3411@cumc.columbia.edu) or David D. Ho (dh2994@cumc.columbia.edu), Columbia University Vagelos College of Physicians and Surgeons, 701 W. 168th Street, New York, NY 10032, USA.

bioRxiv preprint doi: https://doi.org/10.1101/2022.05.26.493517; this version posted May 26, 2022. The copyright holder for this preprint (which was not certified by peer review) is the author/funder. All rights reserved. No reuse allowed without permission.

Abstract

The Omicron subvariant BA.2 accounts for a large majority of the SARS-CoV-2 infection worldwide today[1]. However, its recent descendants BA.2.12.1 and BA.4/5 have surged dramatically to become dominant in the United States and South Africa, respectively[2,3]. That these novel Omicron subvariants carry additional mutations in their spike proteins raises concerns that they may further evade neutralizing antibodies, thereby further compromising the efficacy of our COVID-19 vaccines and therapeutic monoclonals. We now report findings from a systematic antigenic analysis of these surging Omicron subvariants. BA.2.12.1 is only modestly (1.8-fold) more resistant to sera from vaccinated and boosted individuals than BA.2. On the other hand, BA.4/5 is substantially (4.2-fold) more resistant and thus more likely to lead to vaccine breakthrough infections. Mutation at spike residue L452 found in both BA.2.12.1 and BA.4/5 facilitates escape from some antibodies directed to the so-called Class 2 and Class 3 regions of the receptor-binding domain (RBD)[4]. The F486V mutation found in BA.4/5 facilitates escape from certain Class 1 and Class 2 antibodies to the RBD but compromises the spike affinity for the cellular receptor ACE2. The R493Q reversion mutation, however, restores receptor affinity and consequently the fitness of BA.4/5. Among therapeutic antibodies authorized for clinical use, only bebtelovimab (LY-COV1404) retains full potency against both BA.2.12.1 and BA.4/5. The Omicron lineage of SARS-CoV-2 continues to evolve, successively yielding subvariants that are not only more transmissible but also more evasive to antibodies.

bioRxiv preprint doi: https://doi.org/10.1101/2022.05.26.493517; this version posted May 26, 2022. The copyright holder for this preprint (which was not certified by peer review) is the author/funder. All rights reserved. No reuse allowed without permission.

Main text

SARS-CoV-2 Omicron (B.1.1.529) variant continues to dominate the COVID-19 pandemic. Globally, the BA.2 subvariant has rapidly replaced previous subvariants BA.1 and BA.1.1 (Fig. 1a). The recent detection and dramatic expansion of three new Omicron subvariants have raised concerns. BA.2.12.1 emerged in the United States in early February and expanded substantially in the northeast region that includes New York (Fig. 1a), where it now accounts for over 70% of all new SARS-CoV-2 infections[3]. BA.4 and BA.5 emerged in South Africa in January and rapidly became dominant there with a combined frequency of over 88%[1]. These new Omicron subvariants have been detected worldwide, albeit at low levels presently. However, their growth trajectories in the U.S. and South Africa indicate a significant transmission advantage that will likely result in further expansion, as is being observed in countries such as Portugal (Fig. 1a). Phylogenetically, these new subvariants evolved independently from BA.2 (Fig. 1b). The spike protein of BA.2.12.1 contains L452Q and S704L alterations in addition to the known mutations in BA.2, whereas the spike proteins of BA.4 and BA.5 are identical, each with four additional alterations: Del69-70, L452R, F486V, and R493Q, a reversion mutation (Fig. 1c). The location of several of these mutations within RBD of the spike protein (Extended Data Fig. 1) raises the specter that BA.2.12.1 and BA.4/5 may have evolved to further escape from neutralizing antibodies.

Neutralization by monoclonal antibodies

To understand antigenic differences of BA.2.12.1 and BA.4/5 from previous Omicron subvariants (BA.1, BA.1.1, and BA.2) and the wild-type SARS-CoV-2 (D614G), we produced each pseudovirus and then assessed the sensitivity of each pseudovirus to neutralization by a panel of 21 monoclonal antibodies (mAbs) directed to known neutralizing epitopes on the viral spike. Among these, 19 target the four epitope classes in RBD[4], including REGN10987 (imdevimab)[5], REGN10933 (casirivimab)[5], COV2-2196 (tixagevimab)[6], COV2-2130 (cilgavimab)[6], LY-CoV555 (bamlanivimab)[7], CB6 (etesevimab)[8], Brii-196 (amubarvimab)[9], Brii-198 (romlusevimab)[9], S309 (sotrovimab)[10], LY-CoV1404 (bebtelovimab)[11], ADG-2[12], DH1047[13], S2X259[14], CAB-A17[15] and ZCB11[16], as well as 1-20, 2-15, 2-7[17] and 10-40[18] from our group. Two other mAbs, 4-18 and 5-7[17], target the N-terminal domain (NTD). Our findings are shown in Fig. 2a, as well as in Extended Data Figs. 2 & 3. Overall, 18 and 19 mAbs lost neutralizing activity completely or partially against BA.2.12.1 and BA.4/5, respectively. Neutralization profiles were similar for BA.2 and BA.2.12.1

bioRxiv preprint doi: https://doi.org/10.1101/2022.05.26.493517; this version posted May 26, 2022. The copyright holder for this preprint (which was not certified by peer review) is the author/funder. All rights reserved. No reuse allowed without permission.

except for three Class 3 RBD mAbs (Brii-198, REGN10987, and COV2-2130) that were either inactive or further impaired against the latter subvariant. Compared to BA.2 and BA.2.12.1, BA.4/5 showed substantially greater neutralization resistance to two Class 2 RBD mAbs (ZCB11 and COV2-2196) as well as modest resistance to two Class 3 RBD mAbs (REGN10987 and COV2-2130). Collectively, these differences suggest that mutations in BA.2.12.1 confer greater evasion from antibodies to RBD Class 3 region, whereas mutations in BA.4/5 confer greater evasion from antibodies to RBD Class 2 and Class 3 regions. Only four mAbs (CAB-A17, COV2-2130, 2-7, and LY-COV1404) retained good in vitro potency against both BA.2.12.1 and BA.4/5 with IC_{50} below 0.1 μg/mL. Importantly, among these four mAbs, only LY-COV1404 or bebtelovimab is authorized for therapeutic use in the clinic. For antibody combinations previously authorized or approved for clinical use, all showed a substantial loss of activity in vitro against BA.2.12.1 and BA.4/5.

To identify the mutations in BA.2.12.1 and BA.4/5 that confer antibody resistance, we assessed the neutralization sensitivity of pseudoviruses carrying each of the point mutations in the background of D614G or BA.2 to the aforementioned panel of mAbs and combinations. Detailed findings are presented in Extended Data Figs. 4-6, and most salient results are highlighted in Fig. 2b and discussed here. Substitutions (M, R, and Q) at residue L452, previously found in the Delta and Lambda variants[19,20], conferred resistance largely to Classes 2 and 3 RBD mAbs, with L452R being the more detrimental mutation. F486V broadly impaired the neutralizing activity of several Class 1 and Class 2 RBD mAbs. Notably, this mutation decreased the potency of ZCB11 by >2000-fold. In contrast, the reversion mutation R493Q sensitized BA.2 to neutralization by several Class 1 and Class 2 RBD mAbs. This finding is consistent with our previous study[21] showing that Q493R found in the earlier Omicron subvariants mediated resistance to the same set of mAbs. L452, F486, and Q493, situated at the top of RBD, are among the residues most commonly targeted by SARS-CoV-2 neutralizing mAbs whose epitopes have been defined (Fig. 2c). In silico structural analysis showed that both L452R and L452Q caused steric hindrance to the binding by Class 2 RBD mAbs. One such example is shown for LY-CoV555 (Fig. 2d), demonstrating the greater clash because of the Arginine substitution and explaining why this particular mutation led to a larger loss of virus-neutralizing activity (Fig. 2b). Structural modeling

bioRxiv preprint doi: https://doi.org/10.1101/2022.05.26.493517; this version posted May 26, 2022. The copyright holder for this preprint (which was not certified by peer review) is the author/funder. All rights reserved. No reuse allowed without permission.

of the F486V again revealed steric hindrance to binding by Class 2 RBD mAbs such as REGN10933, LY-CoV555, and 2-15 caused by the Valine substitution (Fig. 2e).

Affinity to human ACE2

Epidemiological data clearly indicate that both BA.2.12.1 and BA.4/5 are very transmissible (Fig. 1a); however, the additional mutations at the top of RBD (Fig. 2c) of these subvariants raises the possibility of a significant loss of affinity for the viral receptor, human ACE2 (hACE2), as has been reported by one group[22]. We therefore measured the binding affinity of purified spike proteins of D614G and major Omicron subvariants (Extended Data Fig. 7) to dimeric hACE2 using surface plasmon resonance (SPR). The spike proteins of the Omicron subvariants exhibited similar binding affinities to hACE2, with K_D values ranging from 1.66 nM for BA.4/5 to 2.36 nM for BA.2.12.1 to 2.79 nM for BA.1.1 (Fig. 3a). Impressively, despite having $\geq$17 mutations in the RBD to escape antibody neutralization, BA.2.12.1 and BA.4/5 also evolved concurrently to gain a slightly higher affinity for the receptor than an ancestral SARS-CoV-2, D614G (K_D 5.20 nM).

To support the findings by SPR and to probe the role of point mutations in hACE2 binding, we tested BA.2, BA.2.12.1, and BA.4/5 pseudoviruses, as well as pseudoviruses containing key mutations, to neutralization by dimeric hACE2 in vitro. The IC_{50} values were lower for BA.4/5 and BA.2.12.1 than that of BA.2 (Fig. 3b), again indicating that these two emerging Omicron subvariants have not lost receptor affinity. Our results also showed that the F486V mutation compromised receptor affinity, as previously reported[23], while the R493Q reversion mutation improved receptor affinity. To structurally interpret these results, we modeled F486V and R493Q mutations based on the crystal structure of BA.1-RBD-hACE2 complex[24] overlaid with ligand-free BA.2 RBD (PDB: 7U0N and 7UB0). This analysis found that both R493 and F486 are conformationally similar between BA.1 and BA.2, and F486V led to a loss of interaction with a hydrophobic pocket in hACE2 (Fig. 3c). On the other hand, the R493Q reversion mutation restored a hydrogen bond with H34 and avoided the charge repulsion by K31, seemingly having the opposite effect of F486V. Interestingly, the mutation frequency at F486 had been exceedingly low (<10E-5) until the emergence of BA.4/5 (Extended Data Table 1), probably because of a compromised receptor affinity. Taken together, our findings in Figs. 2 and 3 suggest that F486V

bioRxiv preprint doi: https://doi.org/10.1101/2022.05.26.493517; this version posted May 26, 2022. The copyright holder for this preprint (which was not certified by peer review) is the author/funder. All rights reserved. No reuse allowed without permission.

allowed BA.4 and BA.5 to extend antibody evasion while R493Q compensated for their fitness loss.

Neutralization by polyclonal sera

We next assessed the extent of BA.2.12.1 and BA.4/5 resistance to neutralization by sera from four different clinical cohorts. Sera from persons immunized with only two doses of COVID-19 mRNA vaccines were not examined because most of them could not neutralize earlier Omicron subvariants[21,25]. Instead, we measured serum neutralizing activity for persons who received three shots of mRNA vaccines (boosted), individuals who received mRNA vaccines before or after non-Omicron infection, and patients with either BA.1 or BA.2 breakthrough infection after vaccination. Their clinical information is described in Extended Data Table 2, and the serum neutralization profiles are presented in Extended Data Fig. 8 and the 50% inhibitory dose (ID_{50}) titers are summarized in Fig. 4a. For the "boosted" cohort, neutralization titers were noticeably lower (4.6-fold to 6.2-fold) for BA.1, BA.1.1, and BA.2 compared to D614G (Fig. 4b), as previously reported[21,25]. Titers for BA.2.12.1 and BA.4/5 were even lower, by 8.1-fold and 19.2-fold, respectively, relative to D614G, and by 1.8-fold and 4.2-fold, respectively, relative to BA.2. A similar trend was observed for serum neutralization for the other cohorts, with the lowest titers against BA.4/5, followed next by titers against BA.2.12.1. Relative to BA.2, BA.2.12.1 and BA.4/5 showed 1.2-fold to 1.4-fold and 1.6-fold to 4.3-fold, respectively, greater resistance to neutralization by sera from these individuals who had both mRNA vaccination and SARS-CoV-2 infection.

We also conducted serum neutralization assays on pseudoviruses containing point mutations found in BA.2.12.1 or BA.4/5 in the background of BA.2. Del69-70, L452M/R/Q, and F486V each modestly (1.1-fold to 2.4-fold) decreased the neutralizing activity of sera from all cohorts, while the R493Q reversion mutation modestly (~1.5-fold) enhanced the neutralization (Fig. 4c and Extended Data Fig. 9). S704L, a mutation close to the S1/S2 cleavage site, did not appreciably alter the serum neutralization titers against BA.2. For "boosted" serum samples, the impact of each point mutant on neutralization resistance was quantified and summarized in Fig. 4b.

bioRxiv preprint doi: https://doi.org/10.1101/2022.05.26.493517; this version posted May 26, 2022. The copyright holder for this preprint (which was not certified by peer review) is the author/funder. All rights reserved. No reuse allowed without permission.

Using these serum neutralization results, we then constructed a graphic display to map antigenic distances among D614G, various Omicron subvariants, and individual point mutants for just the "boosted" samples to avoid confounding effects from differences in clinical histories in the other cohorts. The resultant antigenic cartography (Fig. 4d) shows that BA.1, BA.1.1, and BA.2 are approximately equidistant from D614G, with each about 3-4 antigenic units away. BA.2.12.1 is further away from BA.2 by 1 antigenic unit. Most strikingly, BA.4/5 is 6 antigenic units from the D614G and 4 antigenic units from BA.2. Each of the point mutants Del69-70, L452M/Q/R, and F486V adds antigenic distance from BA.2 and D614G, whereas R493Q has the opposite effect. Overall, this map makes clear that BA.4/5 is substantially more neutralization resistant to sera obtained from vaccinated and boosted individuals, with several mutations contributing to the antibody evasion.

Discussion

We have systematically evaluated the antigenic properties of SARS-CoV-2 Omicron subvariants BA.2.12.1 and BA.4/5, which are rapidly expanding in the United States and South Africa, respectively (Fig. 1a). It is apparent that BA.2.12.1 is only modestly (1.8-fold) more resistant to sera from vaccinated and boosted individuals than the BA.2 subvariant that currently dominates the global pandemic (Figs. 4b). On the other hand, BA.4/5 is substantially (4.2-fold) more resistant, a finding consistent with results recently posted by other groups[2,26]. This antigenic distance is similar to that between the Delta variant and the ancestral virus[27] and thus is likely to lead to more breakthrough infections in the coming months. A key question now is whether BA.4/5 would out-compete BA.2.12.1, which poses less of an antigenic threat. The answer should be forthcoming soon in "battlegrounds" where both subvariants are already present and expanding, such as New York. Epidemiologically, since both of these two Omicron subvariants have a clear advantage in transmission, it is therefore not surprising that their abilities to bind the hACE2 receptor remain robust (Fig. 3a) despite numerous mutations in the spike protein. In fact, BA.4/5 may have slightly higher affinity for the receptor, contrary to suggestions that it might be less fit[22].

Our studies on the specific mutations found in BA.2.12.1 and BA.4/5 show that Del69-70, L452M/R/Q, and F486V could individually contribute to antibody resistance, whereas R493Q

bioRxiv preprint doi: https://doi.org/10.1101/2022.05.26.493517; this version posted May 26, 2022. The copyright holder for this preprint (which was not certified by peer review) is the author/funder. All rights reserved. No reuse allowed without permission.

confers antibody sensitivity (Fig. 4b). Moreover, the data generated using SARS-CoV-2-neutralizing mAbs suggest that a mutation at L452 allows escape from Class 2 and Class 3 RBD antibodies and that the F486V mutation mediates escape from Class 1 and Class 2 RBD antibodies (Fig. 2b). It is not clear how Del69-70, a mutation previously seen in the Alpha variant[28], contributes to antibody resistance except for the possible evasion from certain neutralizing antibodies directed to the NTD. As for the use of clinically authorized mAbs to treat or block infection by BA.2.12.1 or BA.4/5, only bebtelovimab (LY-COV1404)[11] retains exquisite potency while the combination of tixagevimab and cilgavimab (COV2-2196 and COV2-2130)[6] shows a modest loss of activity (Fig. 2a).

As the Omicron lineage has evolved over the past few months (Fig. 1b), each successive subvariant has seemingly become better and better at human transmission (Fig. 1a) as well as in antibody evasion[21,29]. It is only natural that scientific attention remains intently focused on each new subvariant of Omicron. However, we must be mindful that each of the globally dominant variants of SARS-CoV-2 (Alpha, Delta, and Omicron) emerged stochastically and unexpectedly. Vigilance in our collective surveillance effort must be sustained.

bioRxiv preprint doi: https://doi.org/10.1101/2022.05.26.493517; this version posted May 26, 2022. The copyright holder for this preprint (which was not certified by peer review) is the author/funder. All rights reserved. No reuse allowed without permission.

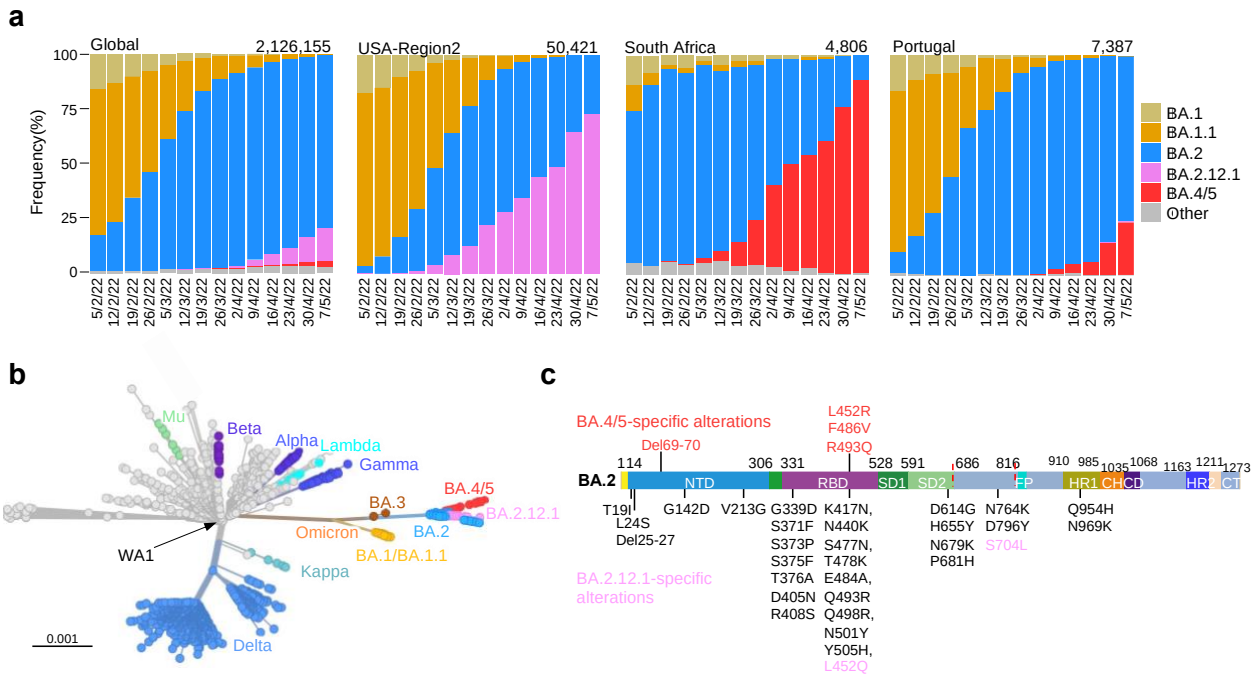

197

198 **Fig. 1 | Prevalence of SARS-CoV-2 Omicron sublineages. a**, Frequencies of BA.1, BA.1.1,
199 BA.2, BA.2.12.1, and BA.4/5 deposited in GISAID. The value in the upper right corner of each
200 box denotes the cumulative number of sequences for all circulating viruses in this time period. The
201 USA-Region2 is defined by the U.S. Department of Health & Human Service, including New
202 York, New Jersey, Puerto Rico and the Virgin Islands. **b**, Unrooted phylogenetic tree of Omicron
203 and its sublineages along with other major SARS-CoV-2 variants. **c**, Key spike mutations found
204 in BA.2, BA.2.12.1, BA.4, and BA.5. Del, deletion.

bioRxiv preprint doi: https://doi.org/10.1101/2022.05.26.493517; this version posted May 26, 2022. The copyright holder for this preprint (which was not certified by peer review) is the author/funder. All rights reserved. No reuse allowed without permission.

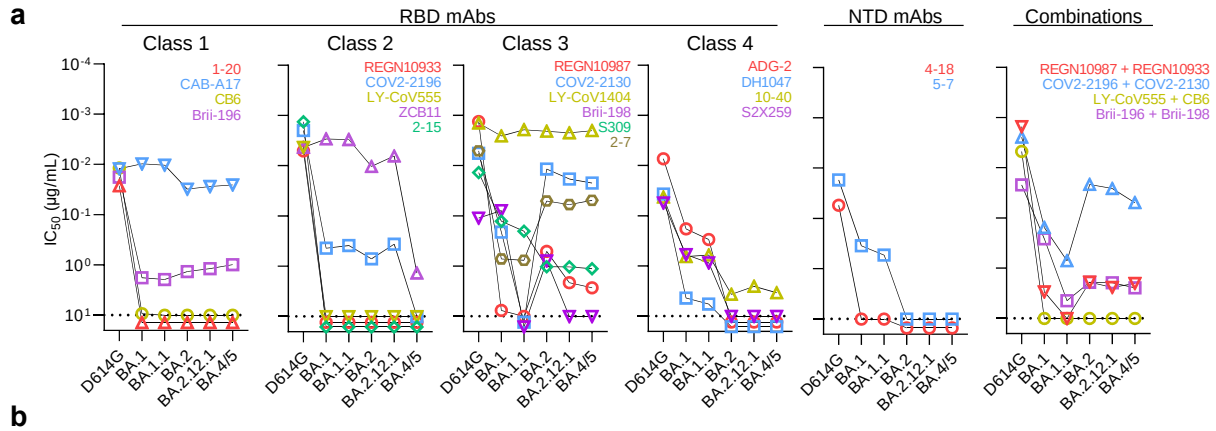

b

Fold change in IC50		RBD mAbs																		NTD mAbs		Combinations			
		Class 1				Class 2					Class 3						Class 4								
		1-20	CAB-A17	CB6	Brii-196	REGN 10933	COV2-2196	LY-CoV555	ZCB11	2-15	REGN 10987	COV2-2130	LY-CoV 1404	Brii-198	S309	2-7	ADG-2	DH1047	10-40	S2X259	4-18	5-7	REGN 10987 + REGN 10933	COV2-2196 + COV2-2130	LY-CoV555 + CB6	Brii-196 + Brii-198
Compared with D614G	D614G-Del69-70	1.3	1.1	1.3	-1.3	-1.0	-1.0	2.0	-1.4	1.3	-1.3	-2.1	-1.3	-1.1	-2.0	-1.0	-1.6	-1.3	-1.7	-1.6	-1.1	-4.6	-1.7	-1.5	-1.1	-1.0
	D614G-L452M	1.5	-1.0	1.5	-1.0	<-1.9	-1.0	-1.8	-1.0	-0.9	-1.5	-1.7	-1.0	-6.9	-2.0	-1.0	-1.5	1.1	1.3	-1.0	-1.1	-1.3	-1.5	-1.1	-1.1	-1.0
	D614G-L452R	-1.2	-1.3	-1.4	-1.5	<-2.0	-1.0	-2266	-1.1	-16	-2.1	-2.6	-1.2	-27	-1.6	-1.8	-1.3	-1.0	1.4	1.8	1.1	-1.1	-1.3	-1.0	-3.9	-1.3
	D614G-L452Q	-1.3	1.1	-1.0	-1.4	<-2.1	-1.0	-5.3	-1.0	-11	-3.7	-3.8	-1.5	-18	-2.7	-2.2	-1.5	-1.5	-1.8	-1.7	-2.0	-1.6	-2.5	-1.7	-3.0	-1.9
	D614G-F486V	-1.5	-1.2	-8.1	-14	<-10000	<-272	-886	-712	-24	-1.1	-1.4	-1.3	-1.4	-1.0	-0.8	-1.4	1.1	-1.7	-2.2	1.1	-1.0	-4.8	-10	-154	-11
	D614G-S704L	1.3	-1.0	-1.6	-1.2	-1.0	-1.0	-1.0	-1.0	-1.3	-1.6	-3.0	1.2	-1.5	-2.7	-1.6	-1.3	-1.7	-1.9	-1.9	-1.9	-1.1	-1.8	-1.5	-1.5	-1.2
	D614G-L452Q/S704L	-1.3	-1.3	-1.9	-1.6	<-7.2	<-1.5	-8.5	-2.8	-32	-4.2	-4.9	-1.5	-48	-2.0	-3.1	-1.8	-1.4	-2.4	-3.0	-2.0	-2.1	-2.4	-2.1	-3.6	-2.2
Compared with BA.2	BA.2-Del69-70	-1.0	-1.5	-1.0	-2.1	-1.0	1.3	-1.0	1.1	-1.0	1.7	1.1	-1.2	1.6	-1.2	-1.0	-1.0	-1.0	<-2.1	-1.0	-1.0	-1.0	-1.5	-1.0	-1.0	1.2
	BA.2-L452M	-1.0	-1.4	-1.0	1.5	-1.0	1.1	-1.0	-1.5	-1.0	-2.2	-2.8	-1.4	<-16	-1.4	-1.3	-1.0	-1.0	1.1	-1.0	-1.0	-1.0	1.2	-1.0	-1.0	1.4
	BA.2-L452R	-1.0	-1.8	-1.0	-5.1	-1.0	-1.2	-1.0	-1.8	-1.0	-5.7	-4.6	-1.1	<-16	-2.6	1.2	-1.0	-1.0	<-2.1	-1.0	-1.0	-1.0	1.3	-1.8	-1.0	<-6.3
	BA.2-L452Q	-1.0	-1.3	-1.0	-1.3	-1.0	1.6	-1.0	1.5	-1.0	-1.8	-1.9	-1.4	<-16	-1.4	-1.6	-1.0	-1.0	<-2.1	-1.0	-1.0	-1.0	-3.2	-1.5	-1.0	-3.5
	BA.2-F486V	-1.0	-8.6	-1.0	<-7.5	1.0	<-9.4	-1.0	<-2182	-1.0	-3.4	1.1	1.1	-1.4	-1.0	-1.7	-1.0	-1.0	-1.2	-1.0	-1.0	-1.0	-5.0	-1.2	-1.0	-3.4
	BA.2-R493Q	>5.0	2.7	-1.0	41.0	>10	22	-1.0	4.6	-1.0	1.1	-1.7	-1.7	-1.7	-1.2	-1.5	-1.0	-1.0	1.6	-1.0	-1.0	-1.0	2.3	1.8	-1.0	76
	BA.2-S704L	-1.0	-1.2	-1.0	-1.1	-1.0	1.5	-1.0	1.2	-1.0	1.9	-1.1	-1.3	-1.1	-1.4	1.1	-1.0	-1.0	1.9	-1.0	-1.0	-1.0	1.2	1.7	-1.0	2.0
	BA.2-F486V/R493Q	-1.0	1.3	-1.0	3.4	-1.0	<-9.4	-1.0	-1834	-1.0	1.5	1.7	1.6	2.2	1.9	1.4	-1.0	-1.0	1.8	-1.0	-1.0	-1.0	1.7	1.1	-1.0	2.7

>10	>3	<-3	<-10	<-100	<-1000

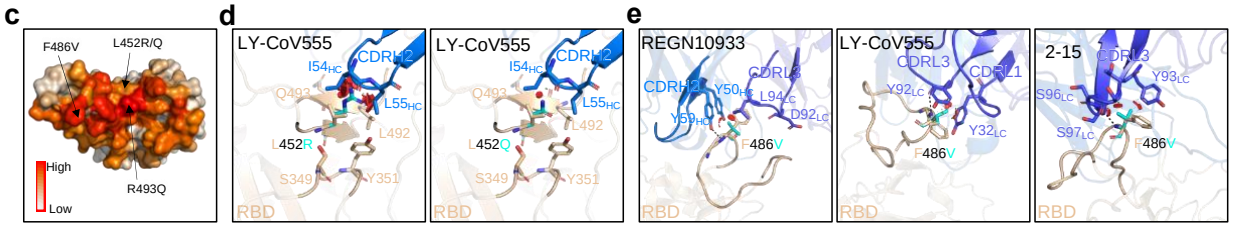

205

206 **Fig. 2 | Resistance of Omicron sublineages to neutralization by monoclonal antibodies. a**,
207 Neutralization of D614G and Omicron sublineages by RBD- and NTD-directed monoclonal
208 antibodies (mAbs). Values above the LOD of 10 μg/mL (dotted line) are arbitrarily plotted to allow
209 for visualization of each sample**. b**, Fold change in IC_{50} values of point mutants relative to D614G
210 or BA.2, with resistance colored red and sensitization colored green. **c**, Location of F486V,
211 L452R/Q, and R493Q on D614G RBD, with the color indicating the per residue frequency
212 recognized by SARS-CoV-2 neutralizing antibodies. Modeling of L452R/Q (**d**) and F486V (**e**)
213 affect class 2 antibody neutralization. The clashes are shown in red plates; the hydrogen bonds are
214 shown in dark dashed lines.

bioRxiv preprint doi: https://doi.org/10.1101/2022.05.26.493517; this version posted May 26, 2022. The copyright holder for this preprint (which was not certified by peer review) is the author/funder. All rights reserved. No reuse allowed without permission.

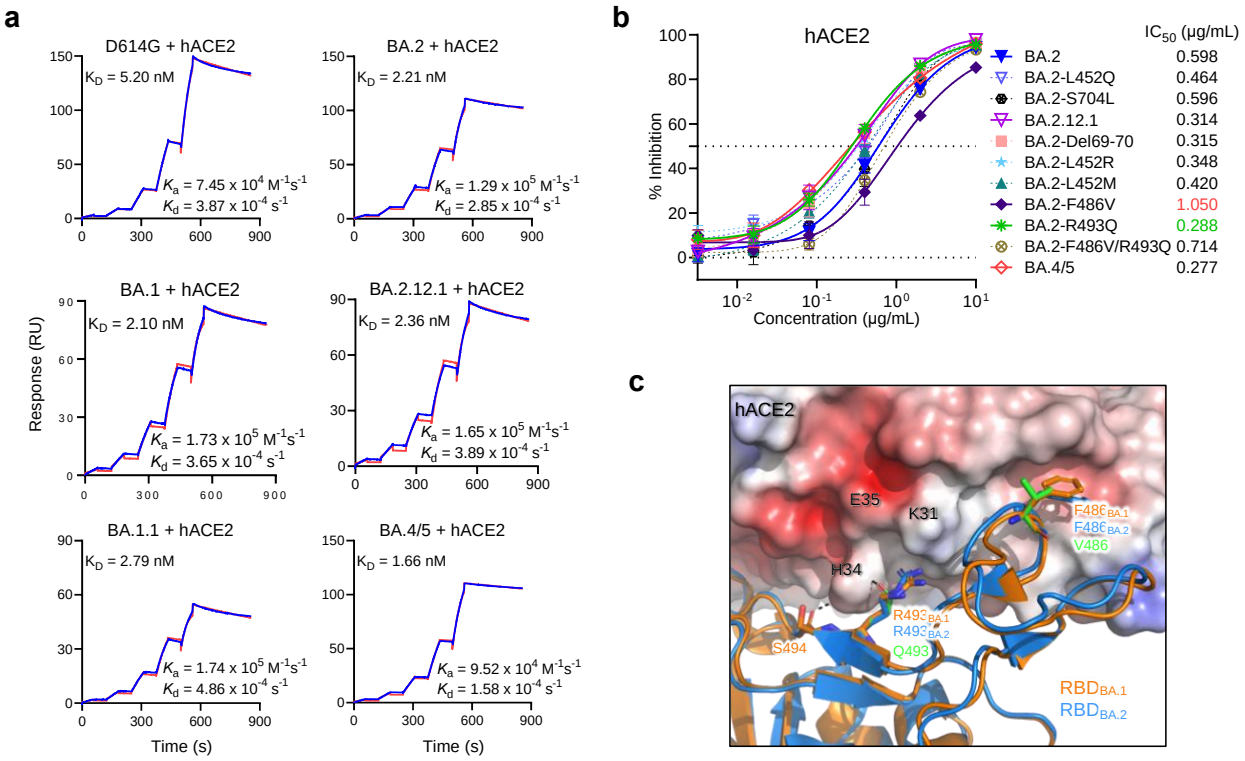

Fig. 3 | Affinity of the spike proteins of SARS-CoV-2 Omicron sublineages to human ACE2 (hACE2). a, Binding affinities of Omicron subvariant S2P spike proteins to hACE2 as measured by SPR. **b**, Sensitivity of pseudotyped Omicron sublineages and the individual mutations in the background of BA.2 to hACE2 inhibition. The hACE2 concentrations resulting in 50% inhibition of infectivity (IC_{50}) are presented. Data are shown as mean ± SEM. **c**, In silico analysis for how R493Q and F486V affect hACE2 binding. The hACE2 surface is shown with charge potential, with red and blue representing negative and positive charges, respectively. Omicron BA.1 RBD in complex with hACE2 was downloaded from PDB 7U0N, and the ligand-free BA.2 RBD was downloaded from PDB 7UB0.

bioRxiv preprint doi: https://doi.org/10.1101/2022.05.26.493517; this version posted May 26, 2022. The copyright holder for this preprint (which was not certified by peer review) is the author/funder. All rights reserved. No reuse allowed without permission.

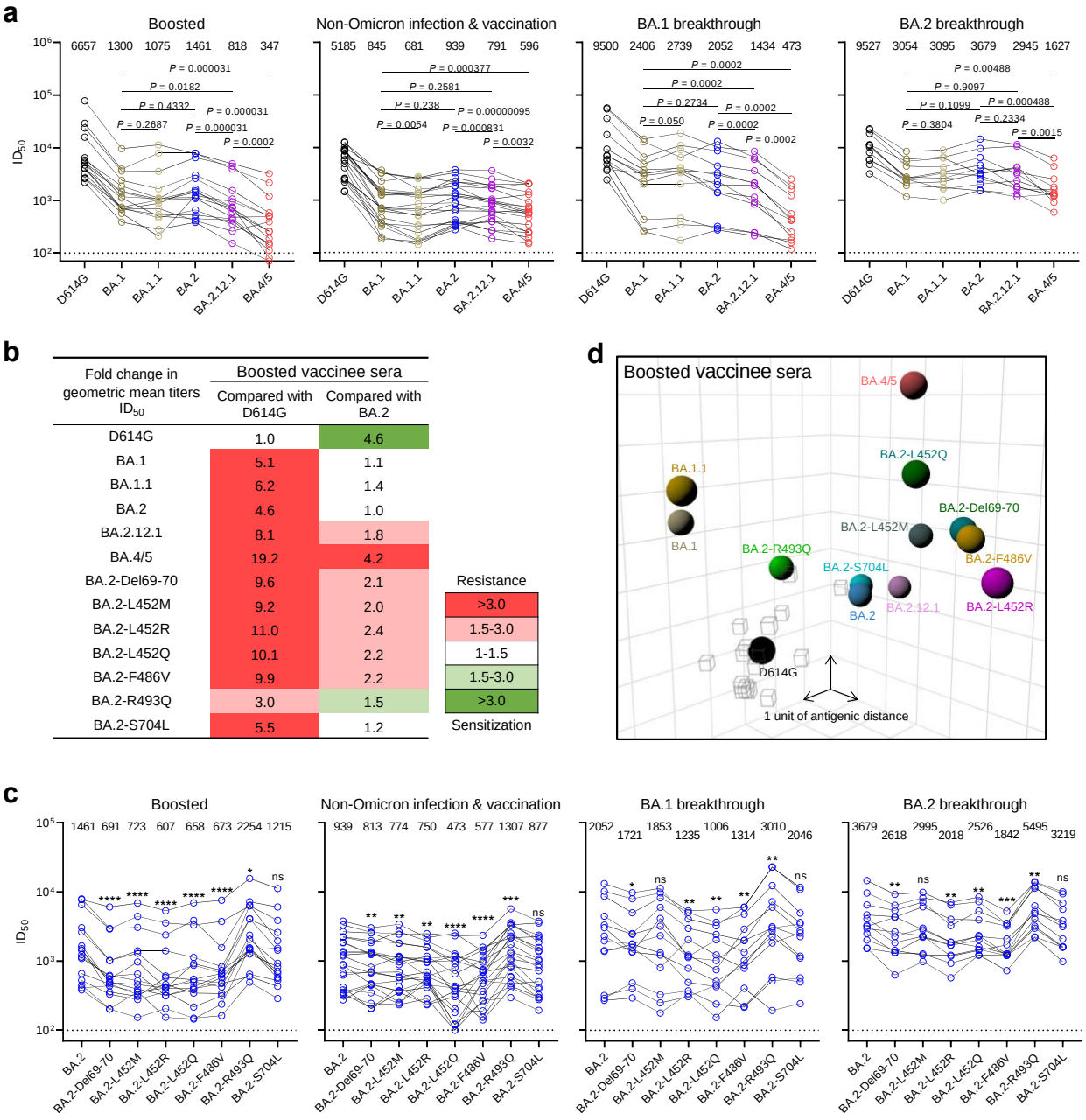

Fig. 4 | BA.2.12.1 and BA.4/5 exhibit greater serum neutralization resistance profiles relative to BA.2. **a**, Neutralization of pseudotyped D614G and Omicron subvariants by sera from 4 different clinical cohorts. **b**, Fold change in geometric mean ID_{50} titers of boosted vaccinee sera relative to D614G and BA.2, with resistance colored red and sensitization colored green. **c**, Serum neutralization of BA.2 pseudoviruses containing single mutations found within BA.2.12.1 and BA.4/5. For all the panels, values above the symbols denote the geometric mean ID_{50} values.

bioRxiv preprint doi: https://doi.org/10.1101/2022.05.26.493517; this version posted May 26, 2022. The copyright holder for this preprint (which was not certified by peer review) is the author/funder. All rights reserved. No reuse allowed without permission.

232 *P* values were determined by using two-tailed Wilcoxon matched-pairs signed-rank tests. *p <
233 0.05, **p < 0.01; ***p < 0.001; ****p < 0.0001; ns - not significant. **d**, Antigenic map based on
234 the neutralization data of boosted vaccinee sera and an interactive map is available online
235 (https://figshare.com/articles/media/OmicronAntigenicMap/19854046).

bioRxiv preprint doi: https://doi.org/10.1101/2022.05.26.493517; this version posted May 26, 2022. The copyright holder for this preprint (which was not certified by peer review) is the author/funder. All rights reserved. No reuse allowed without permission.

References

1 Shu, Y. & McCauley, J. GISAID: Global initiative on sharing all influenza data - from vision to reality. *Euro Surveill* **22**, doi:10.2807/1560-7917.ES.2017.22.13.30494 (2017).

2 Khan, K. *et al.* Omicron sub-lineages BA.4/BA.5 escape BA.1 infection elicited neutralizing immunity. *medRxiv*, doi:10.1101/2022.04.29.22274477 (2022).

3 Centers for Disease Control and Prevention. *COVID Data Tracker*, <https://covid.cdc.gov/covid-data-tracker/#variant-proportions> (2022).

4 Barnes, C. O. *et al.* SARS-CoV-2 neutralizing antibody structures inform therapeutic strategies. *Nature* **588**, 682-687, doi:10.1038/s41586-020-2852-1 (2020).

5 Hansen, J. *et al.* Studies in humanized mice and convalescent humans yield a SARS-CoV-2 antibody cocktail. *Science* **369**, 1010-1014, doi:10.1126/science.abd0827 (2020).

6 Zost, S. J. *et al.* Potently neutralizing and protective human antibodies against SARS-CoV-2. *Nature* **584**, 443-449, doi:10.1038/s41586-020-2548-6 (2020).

7 Jones, B. E. *et al.* The neutralizing antibody, LY-CoV555, protects against SARS-CoV-2 infection in nonhuman primates. *Sci Transl Med* **13**, doi:10.1126/scitranslmed.abf1906 (2021).

8 Shi, R. *et al.* A human neutralizing antibody targets the receptor-binding site of SARS-CoV-2. *Nature* **584**, 120-124, doi:10.1038/s41586-020-2381-y (2020).

9 Ju, B. *et al.* Human neutralizing antibodies elicited by SARS-CoV-2 infection. *Nature* **584**, 115-119, doi:10.1038/s41586-020-2380-z (2020).

10 Pinto, D. *et al.* Cross-neutralization of SARS-CoV-2 by a human monoclonal SARS-CoV antibody. *Nature* **583**, 290-295, doi:10.1038/s41586-020-2349-y (2020).

11 Westendorf, K. *et al.* LY-CoV1404 (bebtelovimab) potently neutralizes SARS-CoV-2 variants. *Cell Rep* **39**, 110812, doi:10.1016/j.celrep.2022.110812 (2022).

12 Rappazzo, C. G. *et al.* Broad and potent activity against SARS-like viruses by an engineered human monoclonal antibody. *Science* **371**, 823-829, doi:10.1126/science.abf4830 (2021).

13 Li, D. *et al.* In vitro and in vivo functions of SARS-CoV-2 infection-enhancing and neutralizing antibodies. *Cell* **184**, 4203-4219 e4232, doi:10.1016/j.cell.2021.06.021 (2021).

14 Tortorici, M. A. *et al.* Broad sarbecovirus neutralization by a human monoclonal antibody. *Nature* **597**, 103-108, doi:10.1038/s41586-021-03817-4 (2021).

15 Sheward, D. J. *et al.* Structural basis of Omicron neutralization by affinity-matured public antibodies. *bioRxiv*, doi:10.1101/2022.01.03.474825 (2022).

16 Zhou, B. *et al.* An elite broadly neutralizing antibody protects SARS-CoV-2 Omicron variant challenge. *bioRxiv*, doi:10.1101/2022.01.05.475037 (2022).

17 Liu, L. *et al.* Potent neutralizing antibodies against multiple epitopes on SARS-CoV-2 spike. *Nature* **584**, 450-456, doi:10.1038/s41586-020-2571-7 (2020).

18 Liu, L. *et al.* An antibody class with a common CDRH3 motif broadly neutralizes sarbecoviruses. *Sci Transl Med*, eabn6859, doi:10.1126/scitranslmed.abn6859 (2022).

19 Planas, D. *et al.* Reduced sensitivity of SARS-CoV-2 variant Delta to antibody neutralization. *Nature* **596**, 276-280, doi:10.1038/s41586-021-03777-9 (2021).

20 Kimura, I. *et al.* The SARS-CoV-2 Lambda variant exhibits enhanced infectivity and immune resistance. *Cell Rep* **38**, 110218, doi:10.1016/j.celrep.2021.110218 (2022).

21 Liu, L. *et al.* Striking antibody evasion manifested by the Omicron variant of SARS-CoV-2. *Nature* **602**, 676-681, doi:10.1038/s41586-021-04388-0 (2022).

22 Cao, Y. *et al.* BA.2.12.1, BA.4 and BA.5 escape antibodies elicited by Omicron infection. *bioRxiv*, doi:10.1101/2022.04.30.489997 (2022).

23 Starr, T. N. *et al.* Shifting mutational constraints in the SARS-CoV-2 receptor-binding domain during viral evolution. *bioRxiv*, doi:10.1101/2022.02.24.481899 (2022).

bioRxiv preprint doi: https://doi.org/10.1101/2022.05.26.493517; this version posted May 26, 2022. The copyright holder for this preprint (which was not certified by peer review) is the author/funder. All rights reserved. No reuse allowed without permission.

24 Geng, Q. *et al.* Structural Basis for Human Receptor Recognition by SARS-CoV-2 Omicron Variant BA.1. *J Virol* **96**, e0024922, doi:10.1128/jvi.00249-22 (2022).

25 Iketani, S. *et al.* Antibody evasion properties of SARS-CoV-2 Omicron sublineages. *Nature* **604**, 553-556, doi:10.1038/s41586-022-04594-4 (2022).

26 Tuekprakhon, A. *et al.* Further antibody escape by Omicron BA.4 and BA.5 from vaccine and BA.1 serum. *bioRxiv*, doi:10.1101/2022.05.21.492554 (2022).

27 Rössler, A. *et al.* BA.2 omicron differs immunologically from both BA.1 omicron and pre-omicron variants. *medRxiv*, doi:10.1101/2022.05.10.22274906 (2022).

28 Wang, P. *et al.* Antibody resistance of SARS-CoV-2 variants B.1.351 and B.1.1.7. *Nature* **593**, 130-135, doi:10.1038/s41586-021-03398-2 (2021).

29 Yu, J. *et al.* Neutralization of the SARS-CoV-2 Omicron BA.1 and BA.2 Variants. *N Engl J Med* **386**, 1579-1580, doi:10.1056/NEJMc2201849 (2022).

30 Wrapp, D. *et al.* Cryo-EM structure of the 2019-nCoV spike in the prefusion conformation. *Science* **367**, 1260-1263, doi:10.1126/science.abb2507 (2020).

31 Krissinel, E. & Henrick, K. Inference of macromolecular assemblies from crystalline state. *J Mol Biol* **372**, 774-797, doi:10.1016/j.jmb.2007.05.022 (2007).

32 Cerutti, G. *et al.* Structural basis for accommodation of emerging B.1.351 and B.1.1.7 variants by two potent SARS-CoV-2 neutralizing antibodies. *Structure* **29**, 655-663 e654, doi:10.1016/j.str.2021.05.014 (2021).

33 Smith, D. J. *et al.* Mapping the antigenic and genetic evolution of influenza virus. *Science* **305**, 371-376, doi:10.1126/science.1097211 (2004).

bioRxiv preprint doi: https://doi.org/10.1101/2022.05.26.493517; this version posted May 26, 2022. The copyright holder for this preprint (which was not certified by peer review) is the author/funder. All rights reserved. No reuse allowed without permission.

Methods

Data reporting

No statistical methods were used to predetermine sample size. The experiments were not randomized and the investigators were not blinded to allocation during experiments and outcome assessment.

Serum samples

Sera from individuals who received three doses of the mRNA-1273 or BNT162b2 vaccine were collected at Columbia University Irving Medical Center. Sera from individuals who were infected by non-Omicron variants of SARS-CoV-2 in addition to vaccination were collected from January 2021 to September 2021 at Columbia University Irving Medical Center or at the Hackensack Meridian Center for Discovery and Innovation (CDI). Sera from individuals who were infected by Omicron (BA.1 or BA.2) following vaccinations were collected from December 2021 to May 2022 at Columbia University Irving Medical Center. All samples were confirmed for prior SARS-CoV-2 infection status by anti-nucleoprotein (NP) ELISA. All collections were conducted under protocols reviewed and approved by the Institutional Review Board of Columbia University or the Hackensack Meridian Center for Discovery and Innovation. All participants provided written informed consent. Clinical information on the different cohorts of study subjects is provided in Extended Data Table 2.

Monoclonal antibodies

Antibodies were expressed as previously described[17]. Heavy chain variable (VH) and light chain variable (VL) genes for each antibody were synthesized (GenScript), then transfected into Expi293 cells (Thermo Fisher Scientific), and purified from the supernatant by affinity purification using rProtein A Sepharose (GE). REGN10987, REGN10933, COV2-2196, and COV2-2130 were provided by Regeneron Pharmaceuticals; Brii-196 and Brii-198 were provided by Brii Biosciences; CB6 was provided by B. Zhang and P. Kwong (NIH); and ZCB11 was provided by Z. Chen (HKU).

Cell lines

bioRxiv preprint doi: https://doi.org/10.1101/2022.05.26.493517; this version posted May 26, 2022. The copyright holder for this preprint (which was not certified by peer review) is the author/funder. All rights reserved. No reuse allowed without permission.

Expi293 cells were obtained from Thermo Fisher Scientific (A14527); Vero-E6 cells were obtained from the ATCC (CRL-1586); HEK293T cells were obtained from the ATCC (CRL-3216). Cells were purchased from authenticated vendors and morphology was confirmed visually before use. All cell lines tested mycoplasma negative.

Variant SARS-CoV-2 spike plasmid construction

BA.1, BA.1.1, and BA.2 spike-expressing plasmids were generated as previously described[21,25]. Plasmids encoding the BA.2.12.1 and BA.4/5 spikes, as well as the individual and double mutations found in BA.2.12.1 and BA.4/5, were generated using the QuikChange II XL site-directed mutagenesis kit according to the manufacturer's instructions (Agilent). To make the constructs for expression of stabilized soluble S2P spike trimer proteins, 2P substitutions (K986P and V987P) and a "GSAS" substitution of the furin cleavage site (682-685aa in WA1) were introduced into the spike-expressing plasmids[30], and then the ectodomain (1-1208aa in WA1) of the spike was fused with a C-terminal 8x His-tag and cloned into the paH vector. All constructs were confirmed by Sanger sequencing and the sequences of the oligos used are provided in Extended Data Table 3.

Expression and purification of SARS-CoV-2 S2P spike proteins

SARS-CoV-2 S2P spike trimer proteins of the D614G and Omicron subvariants were generated by transfecting Expi293 cells with the S2P spike trimer-expressing constructs using 1 mg mL^{-1} polyethylenimine (PEI) and then purifying from the supernatants five days post-transfection using Ni-NTA resin (Invitrogen) according to the manufacturer's instructions[17]. Each S2P trimer protein (1.5 µg) was analyzed on a 4-12% NuPAGE™ Bis-Tris protein gel (Invitrogen) run at 200 V using MOPS buffer, after which the gel was stained with Coomassie Blue dye.

Surface plasmon resonance

Surface plasmon resonance (SPR) binding assays for human ACE2 binding to SARS-CoV-2 spike were performed using a Biacore T200 biosensor equipped with a Series S CM5 chip (Cytiva), in a running buffer of 10 mM HEPES pH 7.4, 150 mM NaCl, 3 mM EDTA, 0.05% P-20 (Cytiva) at 25 °C. Spike proteins were captured through their C-terminal His-tag over an anti-His antibody surface. These surfaces were generated using the His-capture kit (Cytiva) according to the

bioRxiv preprint doi: https://doi.org/10.1101/2022.05.26.493517; this version posted May 26, 2022. The copyright holder for this preprint (which was not certified by peer review) is the author/funder. All rights reserved. No reuse allowed without permission.

manufacturer's instructions, resulting in approximately 10,000 RU of anti-His antibody over each surface. An anti-His antibody surface without antigen was used as a reference flow cell to remove bulk shift changes from the binding signal.

Binding of human ACE2-Fc protein (Sino Biological) was tested using a three-fold dilution series with concentrations ranging from 2.46 nM to 200 nM. The association and dissociation rates were each monitored for 60 s and 300 s respectively, at 30 µL/min. The bound spike/ACE2 complex was regenerated from the anti-His antibody surface using 10 mM glycine pH 1.5. Blank buffer cycles were performed by injecting running buffer instead of human ACE2-Fc to remove systematic noise from the binding signal. The resulting data was processed and fit to a 1:1 binding model using Biacore Evaluation Software.

Pseudovirus production

Pseudoviruses were produced in the vesicular stomatitis virus (VSV) background, in which the native glycoprotein was replaced by that of SARS-CoV-2 and its variants, as previously described[17]. In brief, HEK293T cells were transfected with a spike expression construct with 1 mg mL^{-1} polyethylenimine (PEI) and cultured overnight at 37 °C under 5% CO_2, and then infected with VSV-G pseudotyped ΔG-luciferase (G*ΔG-luciferase, Kerafast) one day post-transfection. After 2 h of infection, cells were washed three times, changed to fresh medium, and then cultured for approximately another 24 h before the supernatants were collected, clarified by centrifugation, and aliquoted and stored at -80 °C for further use.

Pseudovirus neutralization assay

All viruses were first titrated to normalize the viral input between assays. Heat-inactivated sera or antibodies were first serially diluted in medium in 96-well plates in triplicate, starting at 1:100 dilution for sera and 10 µg mL^{-1} for antibodies. Pseudoviruses were then added and the virus–sample mixture was incubated at 37 °C for 1 h. Vero-E6 cells were then added at a density of 3×10^4 cells per well and the plates were incubated at 37 °C for approximately 10 h. Luciferase activity was quantified using the Luciferase Assay System (Promega) according to the manufacturer's instructions using SoftMax Pro v.7.0.2 (Molecular Devices). Neutralization curves and IC_{50} values were derived by fitting a nonlinear five-parameter dose–response curve to the data in GraphPad Prism v.9.2.

bioRxiv preprint doi: https://doi.org/10.1101/2022.05.26.493517; this version posted May 26, 2022. The copyright holder for this preprint (which was not certified by peer review) is the author/funder. All rights reserved. No reuse allowed without permission.

397

398 **Antibody targeting frequency and mutagenesis analysis for RBD**

399 The SARS-CoV-2 spike structure (6ZGE) used for displaying epitope footprints and mutations
400 within the emerging variants was downloaded from the Protein Data Bank (PDB). Epitope residues
401 were identified using PISA[31] with default parameters, and the RBD residues with non-zero buried
402 accessible surface area were considered epitope residues. For each residue within the RBD, the
403 frequency of antibody recognition was calculated as the number of contact antibodies[32]. The
404 structures of antibody-spike complexes for modeling were also obtained from PDB (7L5B (2-15),
405 6XDG (REGN10933), and 7KMG (LY-CoV555)). PyMOL v.2.3.2 was used to perform
406 mutagenesis and to generate structural plots (Schrödinger).

407

408 **Antigenic cartography**

409 The antigenic distances between SARS-CoV-2 variants were approximated by incorporating the
410 neutralization potency of each serum sample into a previously described antigenic cartography
411 approach[33]. The map was generated by the Racmacs package (https://acorg.github.io/Racmacs/,
412 version 1.1.4) in R with the optimization steps set to 2000, and with the minimum column basis
413 parameter set to “none”.

414

bioRxiv preprint doi: https://doi.org/10.1101/2022.05.26.493517; this version posted May 26, 2022. The copyright holder for this preprint (which was not certified by peer review) is the author/funder. All rights reserved. No reuse allowed without permission.

Acknowledgements

This study was supported by funding from the Gates Foundation, JPB Foundation, Andrew and Peggy Cherng, Samuel Yin, Carol Ludwig, David and Roger Wu, Regeneron Pharmaceuticals, and the NIH SARS-CoV-2 Assessment of Viral Evolution (SAVE) Program. We acknowledge David S. Perlin for providing serum samples from a few COVID-19 patients.

Author contributions

D.D.H. and L.L. conceived this project. Q.W. and L.L. conducted pseudovirus neutralization experiments and purified SARS-CoV-2 spike proteins. Y.G. and Z.S. conducted bioinformatic analyses. Q.W., L.L., and S.I. constructed the spike expression plasmids. Q.W. managed the project. J.Y. and M.W. expressed and purified antibodies. L.L. and Z.L. performed surface plasmon resonance (SPR) assay. M.T.Y., M.E.S., J.Y.C., A.D.B. provided clinical samples. H.M. aided sample collections. Y.H. contributed to discussions. D.D.H. and L.L. directed and supervised the project. Q.W., Y.G., L.L., and D.D.H. analyzed the results and wrote the manuscript.

Competing interests

S.I, J.Y., Y.H., L.L., and D.D.H. are inventors on patent applications (WO2021236998) or provisional patent applications (63/271,627) filed by Columbia University for a number of SARS-CoV-2 neutralizing antibodies described in this manuscript. Both sets of applications are under review. D.D.H. is a co-founder of TaiMed Biologics and RenBio, consultant to WuXi Biologics and Brii Biosciences, and board director for Vicarious Surgical.

Data and materials availability

All data are provided in the manuscript.